STRUCTURAL OPTIMIZATION OF ADVANCED AIRCRAFT STRUCTURES

G. SCHNEIDER *

H. GÖDEL **

D. SENSBURG ***

Messerschmitt-Bölkow-Blohm GmbH.
Airplane Division
P.O. Box 801160, 8 Munich 80
W.-Germany

Abstract

A computer software system called ASAT exists at MBB which allows an automatic design of minimum weight structures. In this paper the application of this system to several structures is described. Another part of the paper deals with a structural layout of a forward swept wing in Carbon Fibre composite.

It is shown that a structural optimization system can be very useful in the preliminary design of an airplane especially when it consists of several modules such as

- static load calculation
- deformations and stress calculation by finite elements
- static aeroelastics
- weight calculation
- unsteady aerodynamic forces
- vibration calculation
- flutter calculation

which all can be used separately and independently.

Introduction

For structural design of modern airplanes the use of optimization computer program is mandatory in order to achieve a minimum weight structure whilst taking into account both strength and aeroelastic requirements.

During a cooperation program [1] with the U.S. Air Force Flight Dynamics Laboratory the MBB company exchanged several computer programs in return for receiving the FASTOP-computer-system [2]. This exchange took place in 1977 and for the last three years the structural dynamic group of MBB has further refined the program and also added a static aeroelastic part to it. This new system is now called ASAT. (Automatische Struktur-Auslegung für Tragflächen). This paper deals with the application of ASAT.

* Aerospace Engineer, Aeroelastic Branch
** Aerospace Engineer, Aeroelastic Branch
*** Head Structural Dynamics

Several structural examples are treated in this paper:

- A simplified structure to show the capabilities of the system (the analysis of this structure was partly sponsored by the ZTL-Research Program of the German Ministry of Defense).
- Aeroelastic efficiency calcs for fin and rudder.
- Structural layout of a carbon fibre composite Delta wing.

Finally the structural layout for a forward swept wing is described which was performed with a MBB computer program. It is shown that the low divergence speed of forward swept surfaces can be raised sufficiently with little weight penalty by laying properly the laminates of a CFC design.

Technical Approach

The ASAT-program is able to size cantilevered or free-free surface structures for flutter speed or strength constraints. It is based on a finite element method. Buckling of elements is considered. Also minimum skin gauges can be a limiting factor for sizing. The aeroelastic efficiencies are calculated directly by using the aerodynamic influence coefficients - no iteration procedure is applied. The mathematical approach can be found in [3] and [4].

Sizing of a Simplified Metal Wing Structure for Strength and Flutter Constraints

In order to try out the computer system a simplified structural model was chosen (Fig. 1). The thickness to chord ratio is constant 5%. The surface is cantilevered.

The conditions which are sizing the skin thickness against buckling are presented in Fig. 2. Two aerodynamic load cases were defined:

- $Ma = 0.9,\ q = 5.52\ \frac{N}{cm^2}\ ,\ \alpha = 8°$
- $Ma = 1.4,\ q = 8.28\ \frac{N}{cm^2}\ ,\ \alpha = 5.5°$

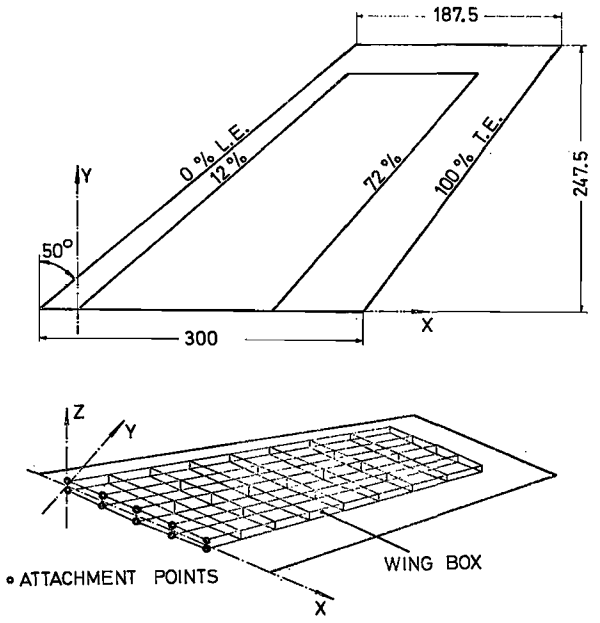

FIG. 1 GEOMETRY AND STRUCTURAL IDEALIZATION

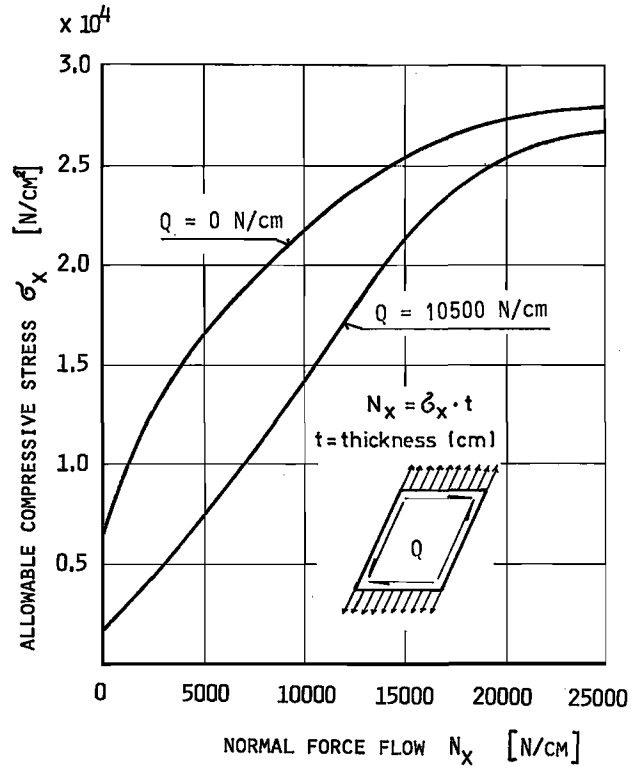

FIG. 2 ALLOWABLE COMPRESSIVE STRESS σ_x AS FUNCTION OF NORMAL FORCE FLOW N_x AND SHEAR FLOW Q

The stationary pressure distributions as calculated by the computer program are shown in Fig. 3. A transformation procedure is implemented which transfers the aerodynamic loads from the panel center to the structural grid points.

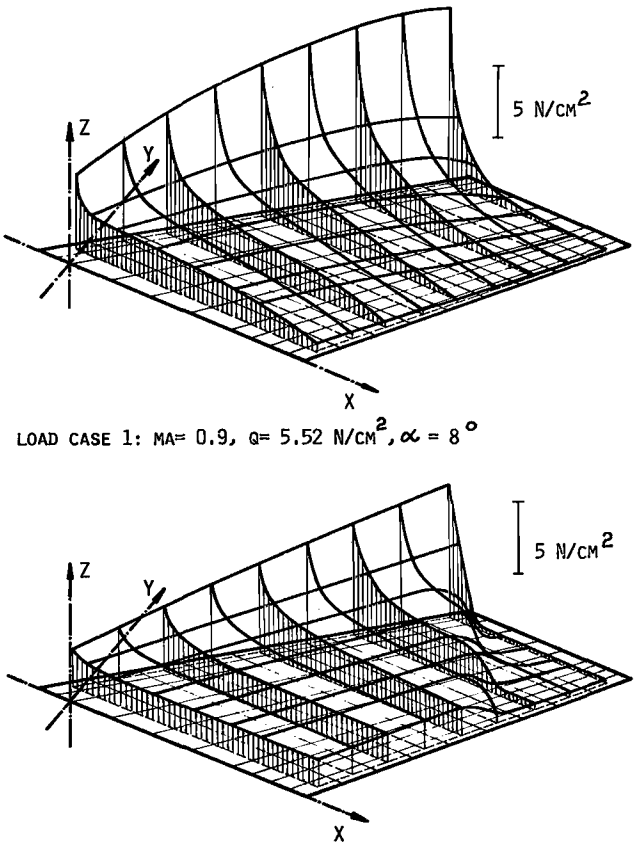

FIG. 3 STATIONARY PRESSURE DISTRIBUTIONS

The optimization process is explained best by Table 1 and 2.

Thicknesses and flutter derivatives for characteristical structural elements for the upper and lower skin are printed for successive steps of the optimization procedure. Initially a constant skin thickness is provided. After three steps of the SOP-module (Struktur Optimierung) a fully stressed design is reached where the last weight change is only 0.7 kg. This is plotted in Table 1.

Weight	Initial weight for constant skin thickness	Iteration Step 1	2	3
kg	51.4	56.7	55.0	54.3

TABLE 1 Weight for structural optimization procedure (SOP)

In Table 2 the iteration procedure is shown for selected structural elements. It starts with the skin thicknessses of step 3 of SOP and then it iterates between FOP (Flatter OPtimierung) to fulfill the required flutter speed with a minimum weight increase and still keeps the fully stressed design by running through SOP.

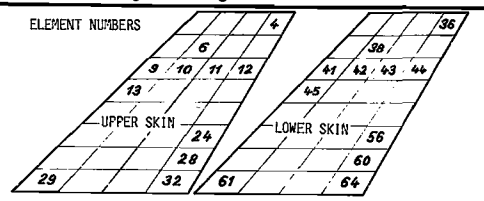

UPPER COVER SKIN

THICKNESS [mm]

Element	Start Value	SOP	FOP	SOP	FOP	SOP	FOP	SOP	FOP	SOP	FOP
4	2.00	0.76	0.76	0.76	0.96	0.96	0.99	0.99	0.96	0.96	0.96
6	2.00	2.78	2.73	2.64	2.63	2.58	2.58	2.56	2.56	2.56	2.56
9	2.00	1.58	1.91	1.91	2.96	2.96	3.73	3.73	3.95	3.95	3.95
10	2.00	2.46	2.34	2.62	2.95	2.95	3.12	3.12	2.97	2.95	2.95
11	2.00	1.72	1.76	1.85	2.72	2.72	3.43	3.43	3.69	3.69	3.69
12	2.00	2.13	2.17	2.29	3.05	3.05	3.53	3.53	3.51	3.51	3.51
13	2.00	2.18	2.28	2.52	3.13	3.13	3.20	3.20	3.13	3.13	3.13
24	2.00	5.84	5.89	5.88	5.88	5.87	5.86	5.85	5.85	5.85	5.85
28	2.00	5.39	5.59	5.47	5.47	5.30	5.23	5.16	5.13	5.12	5.12
29	2.00	1.67	1.54	1.53	1.54	1.60	1.64	1.67	1.69	1.69	1.69
32	2.00	7.82	8.00	7.94	7.94	7.81	7.76	7.70	7.68	7.68	7.68

FLUTTER VELOCITY DERIVATIVES [kts/kg]

4	10.38	13.41	11.09	10.92	11.30
6	2,52	4.09	5.32	5.60	5.58
9	17.82	20.50	16.42	13.79	13.16
10	7.92	10.85	11.56	10.85	10.97
11	12.92	18.47	16.49	14.14	13.58
12	10.39	15.23	13.78	12.13	12.08
13	13.46	13.22	10.79	10.32	10.23
24	0.27	0.62	1.13	1.32	1.32
28	-0.29	-0.15	0.14	0.26	0.27
29	0.90	1.58	2.29	2.51	2.46
32	-0.50	-0.46	-0.34	-0.29	-0.28

LOWER COVER SKIN

THICKNESS [mm]

36	2.00	0.76	0.76	0.76	0.96	0.96	0.99	0.99	0.96	0.96	0.96
38	2.00	0.79	0.80	0.80	0.98	0.98	0.98	0.98	0.98	0.98	0.98
41	2.00	0.76	2.17	2.17	3.92	3.92	4.55	4.55	4.45	4.45	4.45
42	2.00	0.79	1.59	1.59	2.78	2.78	3.38	3.38	3.46	3.46	3.46
43	2.00	0.76	1.84	1.84	3.37	3.37	4.07	4.07	4.14	4.14	4.14
44	2.00	0.76	1.53	1.53	2.73	2.73	3.30	3.30	3.35	3.35	3.35
45	2.00	0.80	1.94	1.94	2.87	2.87	3.08	3.08	2.95	2.95	2.95
56	2.00	3.01	3.10	3.02	3.00	2.88	2.85	2.82	2.81	2.81	2.81
60	2.00	2.84	2.97	2.91	2.90	2.78	2.73	2.69	2.67	2.67	2.67
61	2.00	0.76	0.76	0.76	0.77	0.77	0.82	0.82	0.81	0.81	0.81
64	2.00	4.55	4.43	4.64	4.63	4.51	4.47	4.42	4.40	4.40	4.40

FLUTTER VELOCITY DERIVATIVES [kts/kg]

36	10.19	13.61	10.98	10.96	11.29
38	12.37	12.82	9.96	9.42	9.14
41	100.04	27.81	13.92	11.74	12.23
42	50.07	26.09	15.30	12.85	12.63
43	72.06	28.60	15.03	12.68	12.55
44	49.40	27.31	15.09	12.69	12.49
45	72.78	18.68	11.87	11.30	12.01
56	1.93	2.91	4.10	4.42	4.41
60	-1.01	-0.24	0.96	1.36	1.35
61	6.37	8.82	11.57	12.03	12.16
64	-1.25	-1.11	-0.81	-0.66	-0.63

FINAL STRUCTURAL WEIGHT 64.6 kg

Tab. 1 Optimization Progress for selected structural elements

The elements most important for flutter speed (stiffness change) are underlined. It is interesting to note that for instance the upper skin is mostly designed by strength requirements whereas the lower skin thickness can be used to raise the flutter speed by a stiffness change. After a constant flutter derivative for each important flutter element is reached then the process is finished. Graphically this is shown in Fig. 4.

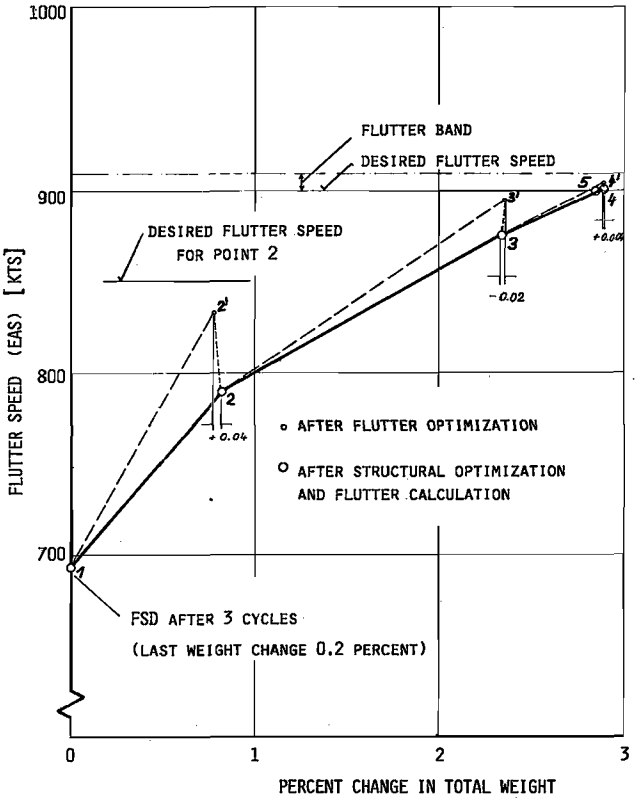

FIG. 4 RESULTS OF REDESIGN STUDY

A flutter speed is calculated for the initial fully stressed design (FSD) being 700 kts. After five iteration steps the desired flutter speed of 900 kts is reached with an increase of less than 3% of total weight. The loss of flutter speed from 2' to 2 and 3' to 3 can be explained this way: The program uses the old vibration modes to get from 1 to 2' but these modes change a little which is reflected in point 2. When the structural changes are smaller and smaller then the modes stay practically the same (see point 4', 4 and 5). In Fig. 5 the elastic deformations before and after optimization are shown.

In Fig. 6 the vibration mode shapes are depicted. From this picture it can be seen that the mode shapes stay almost the same and only the frequencies are changed.

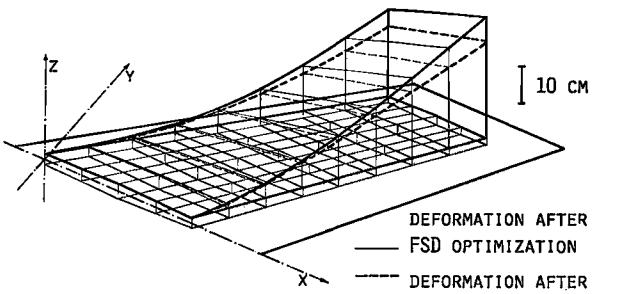

LOAD CASE 1: MA= 0.9, Q= 5.52 N/CM ,α= 8°

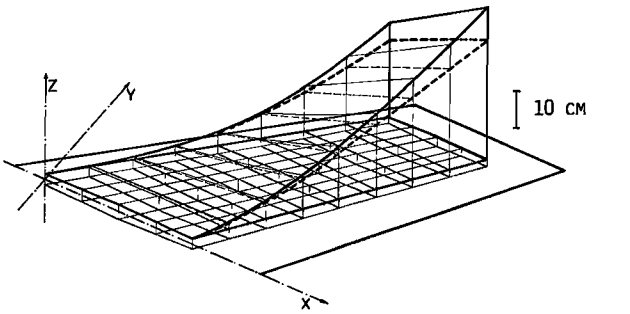

LOAD CASE 2: MA= 1.4, Q= 8.28 N/CM, α = 5.5°

FIG 5 DEFORMATION OF THE STRUCTURE DUE TO LOAD CASE 1 AND 2

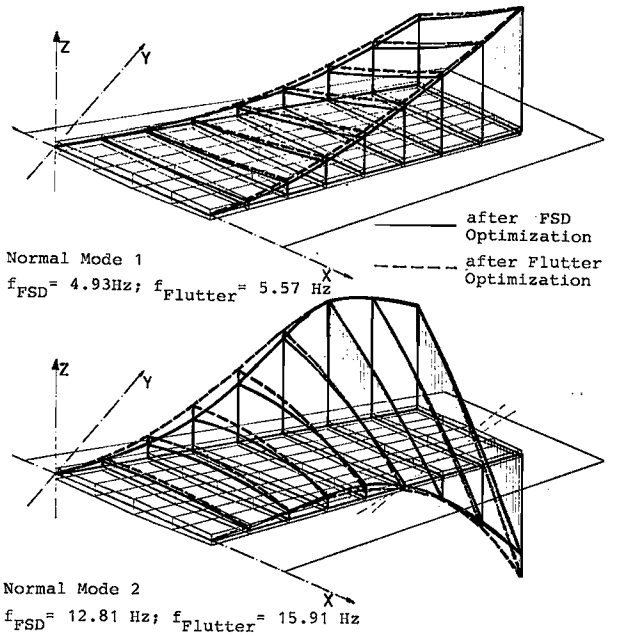

FIG. 6a NORMAL MODES, CALCULATED AFTER INITIAL FSD AND AFTER FLUTTER OPTIMIZATION

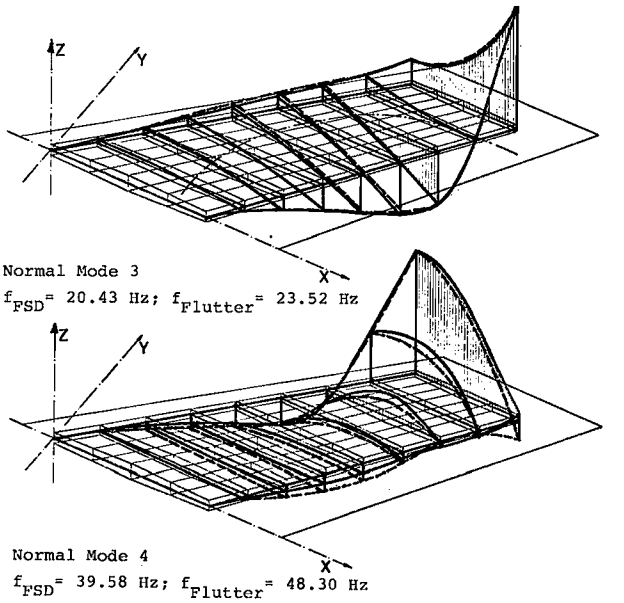

FIG. 6b NORMAL MODES, CALCULATED AFTER INITIAL FSD AND AFTER FLUTTER OPTIMIZATION

The flutter speed increase stems mainly from the frequency separation of mode 1 (bending) and mode 2 (torsion) as shown in Fig. 7.

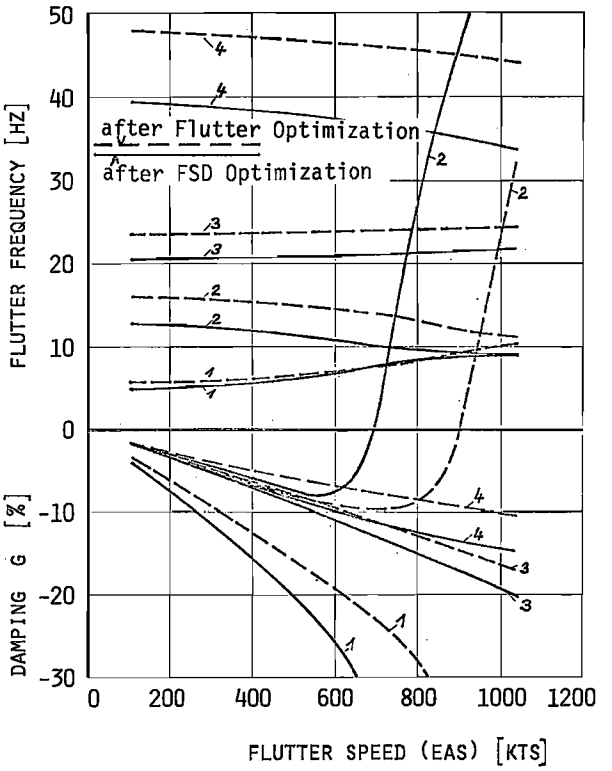

FIG. 7 FLUTTER ANALYSIS

The program FOP has also the possibility to increase flutter speed by mass balancing. Seven mass positions at the outer wing to apply balance masses were provided but the flutter derivatives were so small that this possibility was neglected automatically.

The final results are presented in Fig. 8 and Fig. 9 as skin thicknesses for the upper and lower skin before and after optimization. Also the stress ratios - which should be unity when fully stressed - and the flutter derivatives are shown.

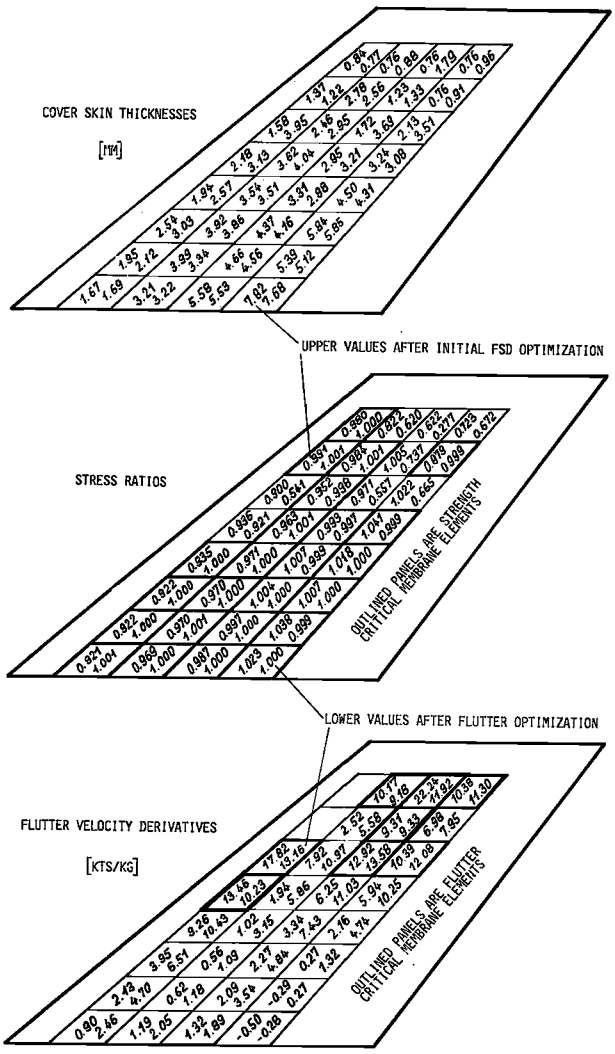

FIG. 8 REDESIGN RESULTS FOR UPPER COVER SKIN

The normal force flow for load case 2 is shown in Fig. 10 as a typical example of the strength calculation.

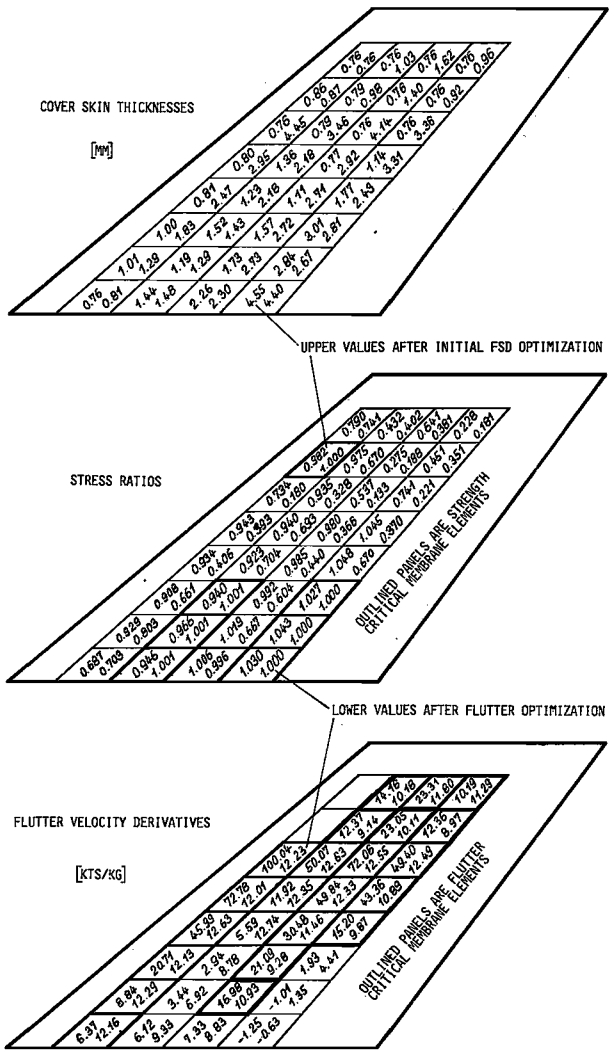

FIG. 9 REDESIGN RESULTS FOR LOWER COVER SKIN

Comparisons for stress calculations with different elements are presented in Fig. 11. This figure proves that with a relative crude element and mesh system good correlation with analyses using more sophisticated elements - such as NASTRAN (triangular membrane with linearly varying stress) - can be achieved. This is an important result because the cruder the idealization can be, the less computer time is needed to run the optimization program.

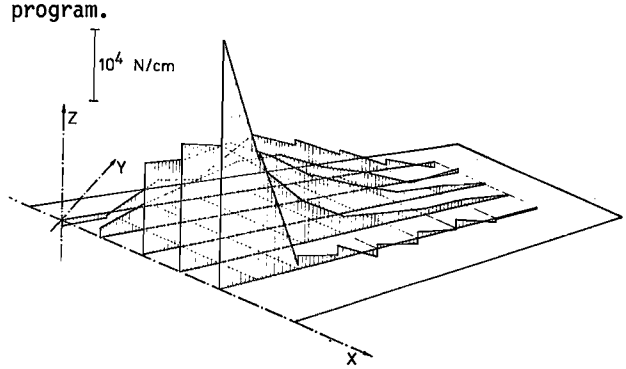

FIG. 10: NORMAL FORCE FLOW IN SPAR DIRECTION FOR LOAD CASE 2

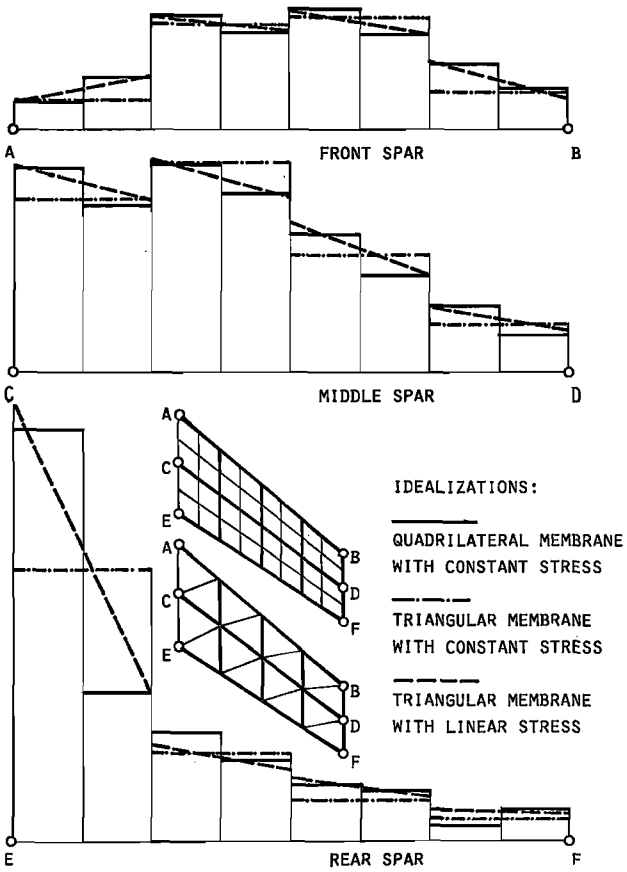

FIG. 11 STRESSES FOR DIFFERENT ELEMENT TYPES AND MESH SYSTEMS

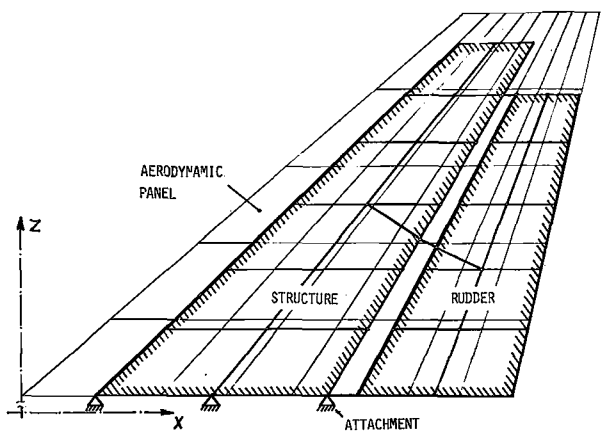

FIG. 12 IDEALIZATION OF A CFC-VERTICAL TAIL

Aeroelastic Efficiency Calculation for a CFC Fin and Rudder

For the structural design of fin and rudder stiffness considerations are overriding and not strength. Also the size of these surfaces is influenced by their aeroelastic efficiency. The program ASAT was used to calculate the efficiency for a fin and rudder of a modern fighter plane. The aeroelastic deformations where calculated directly without using any iteration procedure which is possible because a full matrix of aerodynamic influence coefficient is produced by the aerodynamic module of ASAT.

The properties of CFC where introduced by the stress-strain law.

Fig. 12 shows the structural idealization for a CFC-fin and rudder. Fig. 13 shows the deflections of the structure due to a steady load case.

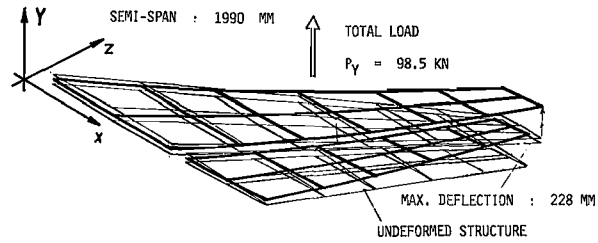

FIG. 13 DEFLECTION DUE TO A STATIC LOAD

Fig. 14 presents relatively large changes in the pressure distributions due to elastic fin deformations especially for the subsonic case.

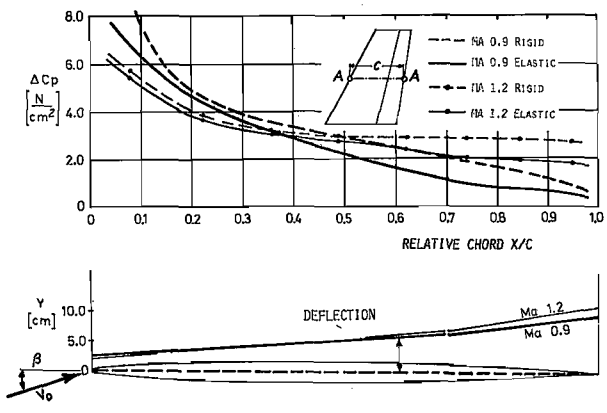

FIG. 14 PRESSURE DISTRIBUTIONS AND DEFORMATIONS AT SECTION A-A DUE TO A FIN ANGLE OF ATTACK β

Fig. 15 is depicting even larger effects on the fin pressure distribution due to rudder angle when elastic effects are considered.

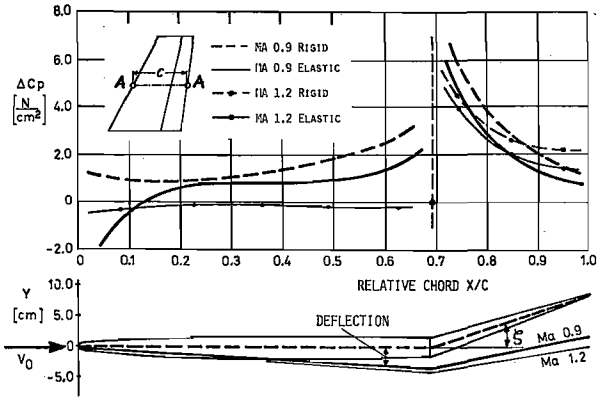

FIG. 15 PRESSURE DISTRIBUTIONS AND DEFORMATIONS AT SECTION A-A DUE TO A RUDDER ROTATION ANGLE

Fig. 16 and Fig. 17 present the aeroelastic effectiveness of fin and rudder and it is shown that the requirements which were postulated by the aerodynamic department can almost be fulfilled.

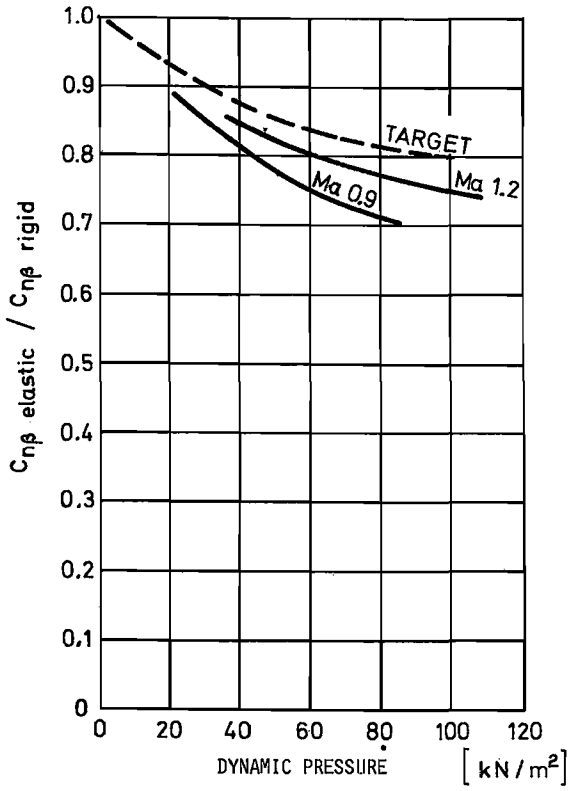

FIG. 16 VERTICAL TAIL AEROELASTIC EFFECTIVENESS

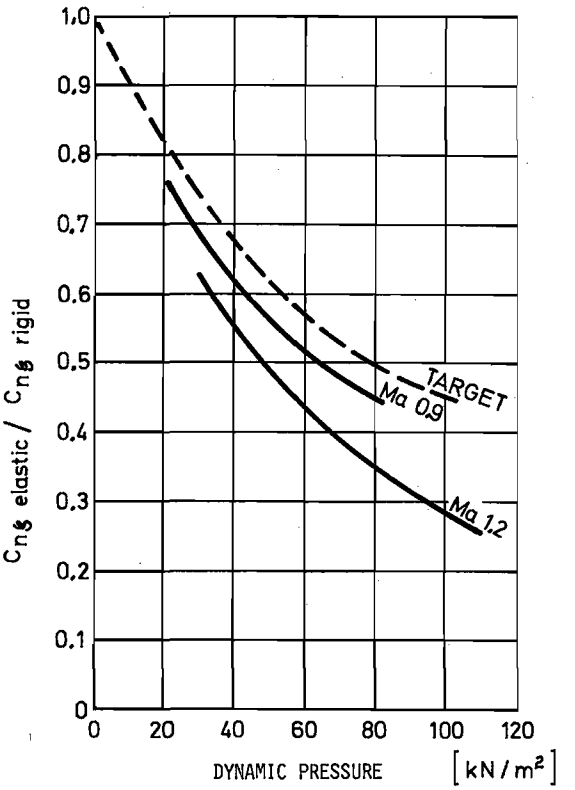

FIG. 17 RUDDER EFFECTIVENESS

Structural Optimization of a CFC-Delta-Wing

For a preliminary design of a CFC-Delta-Wing a structural optimization was performed to achieve a minimum weight structure by retaining sufficient control surface effectiveness. An additional constraint - a certain amount of wing twist off at a high g-manouvre - had to be fulfilled as well [5].

The direction of the laminates were selected in prestudies by the MBB-stress department which have accumulated a lot of experience with the CFC material over the last years [6].

Despite the fact that a huge amount of papers has been published lately about aeroelastic tailoring with CFC it is our opinion that the possibilities for laying the laminates are limited for two major reasons:

- Material properties are only known for specific composites
- Production considerations are dominating.

For these reasons we took the preselected material properties [7] and fed it into the ASAT program as

$$\begin{Bmatrix} \sigma_x \\ \sigma_y \\ \tau_{xy} \end{Bmatrix} = \begin{bmatrix} A_{11} & A_{12} & A_{13} \\ A_{21} & A_{22} & A_{23} \\ A_{31} & A_{32} & A_{33} \end{bmatrix} \cdot \begin{Bmatrix} \varepsilon_x \\ \varepsilon_y \\ \gamma_{xy} \end{Bmatrix}$$

The structure is practically idealized as a thin sandwich plate with the stress carrying capability in the skin. Deformation results for this model were compared with results calculated by the stress group who had a much finer grid and good correlation was achieved.

Calculations were performed for the idealized structure of Fig. 18 and Fig. 19 .

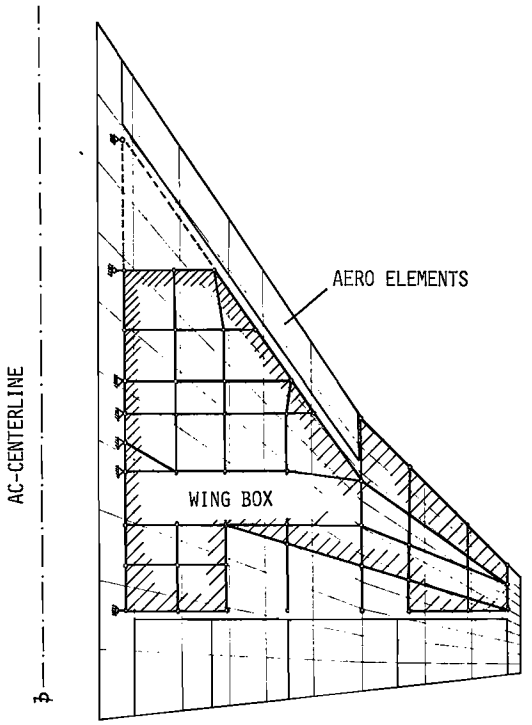

FIG. 18 IDEALIZED DELTA WING FOR STRUCTURAL DESIGN STUDIES

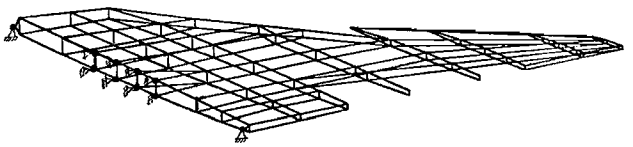

FIG. 19 WING BOX STRUCTURE

The structure is represented as follows:

Grid points	:	106
Degrees of freedom	:	278
Membranes	:	74
Rod elements	:	55
Shear panels	:	67

The final result of these calcs were skin thicknesses adjusted to strength and buckling requirements and the effectivenesses for the control surfaces.

Fig. 20 shows the stress group grid and that one used by ASAT. Only from looking at these pictures one can imagine that local stress concentrations - at attachments for instance - cannot be accounted for by the ASAT-idealization. For this reason it is always necessary to follow up the optimization process with a normal stress analysis to confirm the results.

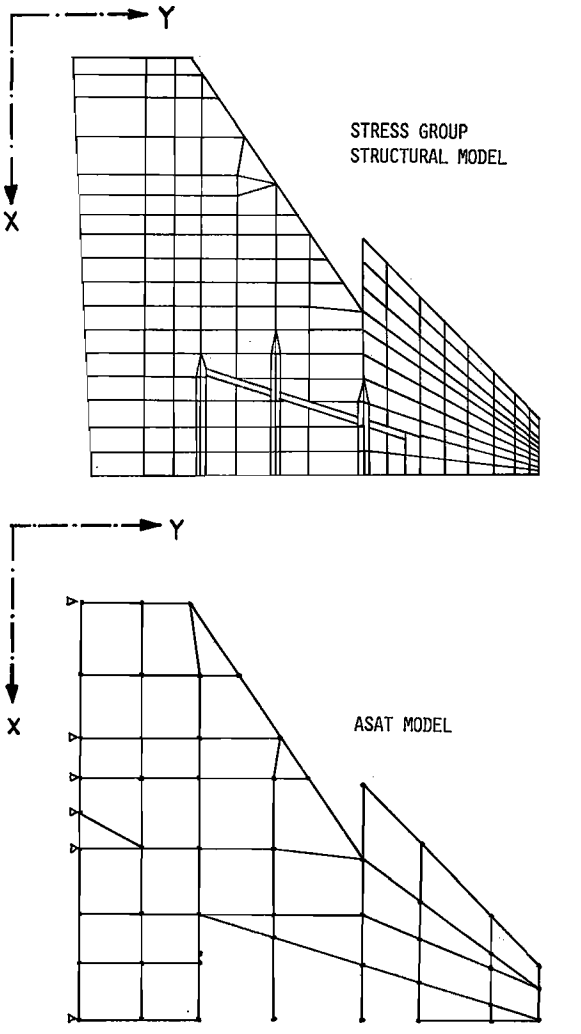

FIG. 20 COMPARISON OF DIFFERENT WING BOX IDEALIZATION

Determination of Loads

Two load cases were chosen according to the definitions of our loads group [8]:

- Load case 1: Symmetrical high g pullout
  This is a manouvre case in the subsonic regime giving the highest shear force and bending moment at the wing root.
- Load case 2:
  This is a roll case in the supersonic flight regime were the aerodynamic center of pressure is backward. This case is not symmetrical (initiated by the ailerons) but was applied two both wings symmetrically.

In order to make the loads calculated by ASAT comparable to the loads from our loads group the wing attitude and aileron angles are somewhat different - the presence of a canard had to be reflected which the ASAT program is not able to consider at the moment.

Results of Deformation Calculations with ASAT and Comparisons

After establishing the structural model and the loads, deformation calculations were performed which match the stress group results very well. Implicitly this is also a prove that comparable loads were used. Fig. 21 shows the vertical deflection along the wing span for load case 1.

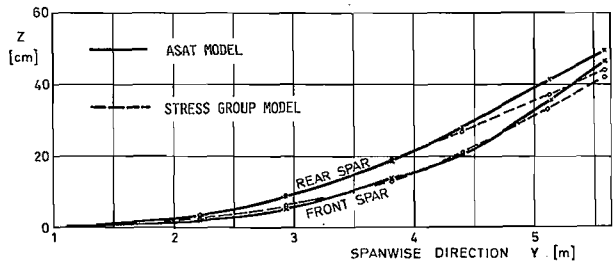

FIG. 21 COMPARISON OF WING DEFLECTIONS

In Fig. 22 the wing twist angle along the span is depicted. The 4° twist off angle at the wing tip fulfills the requirement coming from aerodynamic performance

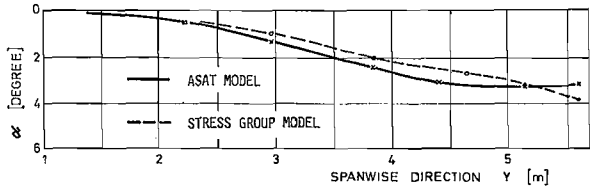

FIG. 22 COMPARISON OF WING TWIST ANGLE α

In Fig. 23 the internal skin load distribution for load case is is presented. From this figure it can be deduced that extreme care must be taken to accomodate such high local forces into the two rear CFC attachments fitted to the fuselage.

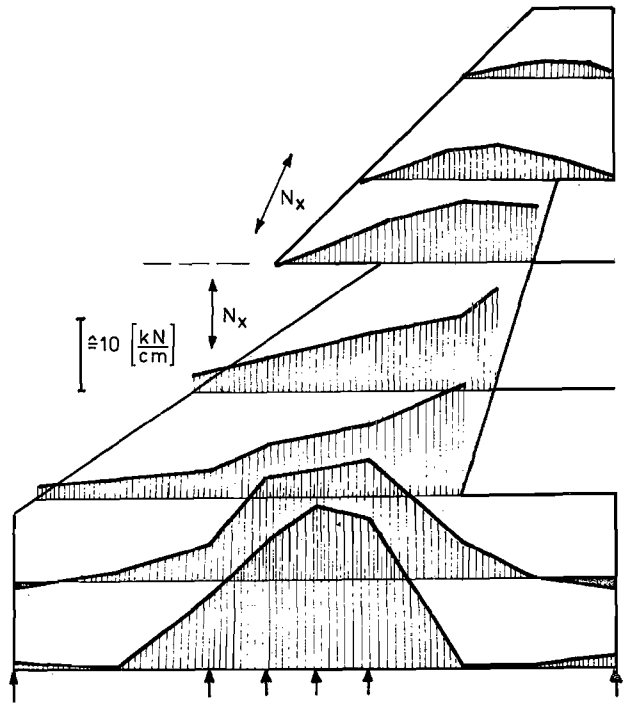

FIG. 23 INTERNAL SKIN LOAD DISTRIBUTION

Results of the Optimization Process

After three steps of the SOP program the skin weight stayed almost constant. The final weight was

Step	Skin Weight [kg]
1	221.7
2	164.4
3	163.9
4	164.1

practically reached after the first step but the convergence had to be proven.

The weight saving amounts to about 5% of the total wing weight which is a very considerable achievement.

Fig. 24 shows the skin thickness distributions before and after structural optimization.

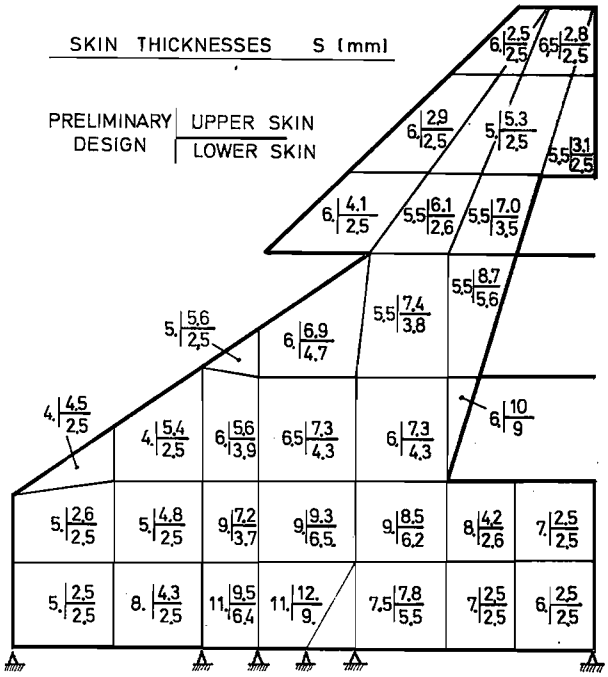

FIG. 24 WEIGHT OPTIMIZED SKIN THICKNESS ACCORDING TO STRENGTH CRITERIA (SUBSONIC AND SUPERSONIC LOAD CASES)

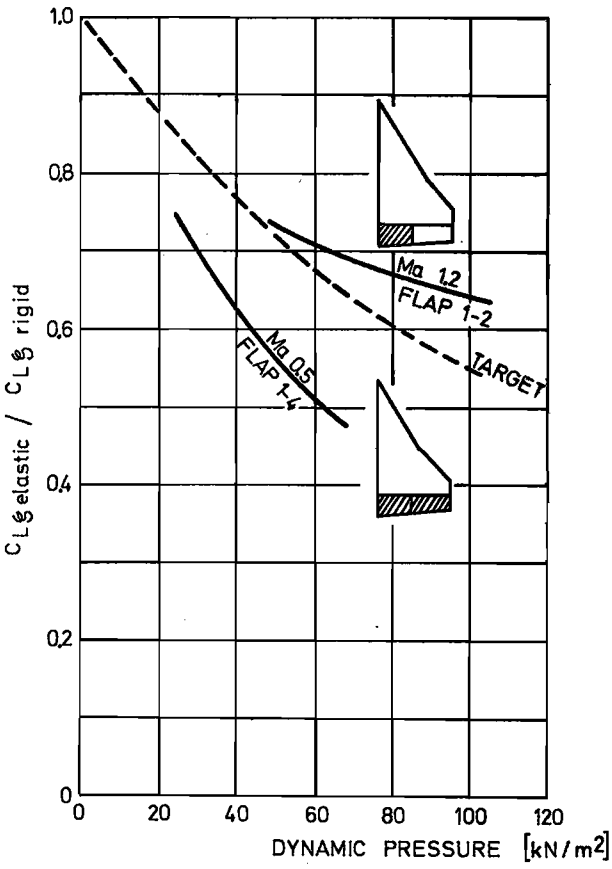

FIG. 25 WING-FLAP CONTROL EFFECTIVENESS

The aeroelastic efficiencies for the aileron are shown in Fig. 25 together with the effectiveness definition to fulfill the roll requirement. For the supersonic case where the roll manouvre is iniated with the two inner flaps only we have higher than required efficiency. For the subsonic pullout manouvre the efficiency for all four flaps is somewhat below the requirement but it still is sufficient.

Structural Design of a CFC Forward Swept Wing (FSW)

Forward swept wings have always attracted designers of high performance airplanes. Aerodynamically there are numerous benefits [9]. The major reason why they have been rejected was their tendency toward static divergence. To overcome this problem for metal structures severe weight penalties occur which more than equalize the aerodynamic benefits.

With the advent of carbon fibre composites it is now possible to raise the static divergence speed sufficiently with little or no weight penalty compared to an aft swept wing.

According to a very valuable publication of T. WEISSHAAR [10] a computer program was developed at MBB which calculates the divergence speeds for various CFC forward swept wings [11]. With this program a structural design study and some comparisons with an aft swept wing equivalent in area were made.

Fig. 26 shows the two wing designs investigated and also the representation by a beam structure with an elastic axis.

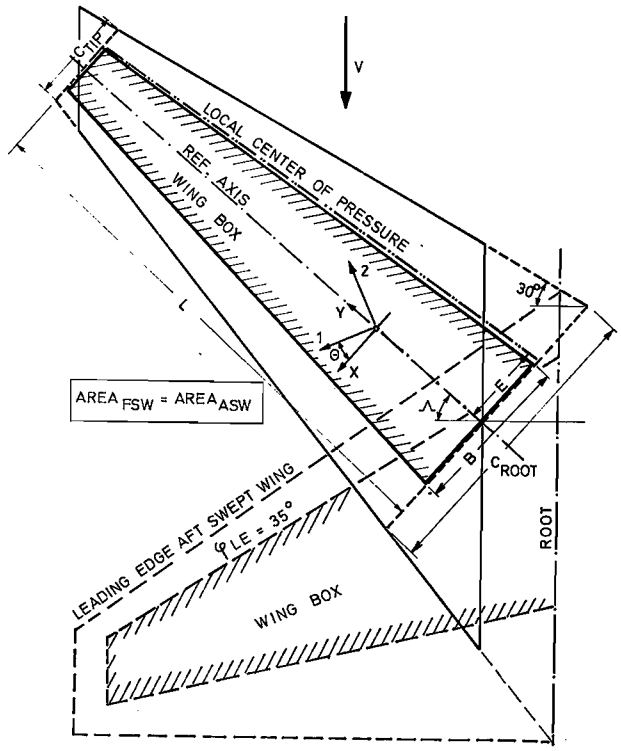

FIG. 26 SIMPLIFIED BEAM MODEL FOR DIVERGENCE STUDIES

In Fig. 27 an attempt is made to explain the divergence tendency of forward swept wings and the reason why it is possible to reduce this tendency when using anisotropic materials.

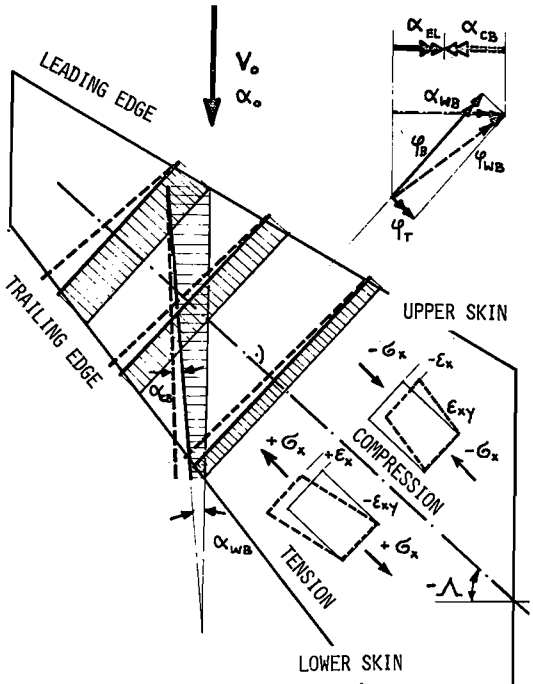

φ_B ANGLE DUE TO WING BENDING MOMENT
φ_T ANGLE DUE TO WING TORSION MOMENT
φ_{WB} TOTAL WING BOX ROTATION
α_{WB} STREAMLINE COMPOSITE OF φ_{WB}
α_{CB} ROTATION DUE TO COMPOSITE BEHAVIOUR
α_{EL} TOTAL ELASTIC ANGLE OF ATTACK

FIG. 27 STRUCTURAL BEHAVIOUR OF A COMPOSITE FORWARD SWEPT WING

When a wing bends under external airloads than the wing sections perpendicular to the elastic axis have the same deflections. For a swept wing this means that the wing twists off (wash-out) in streamwise direction and that it has a wash-in for negative sweep.

Because of the coupling of the normal stresses σ_x which produce a normal strain and a strain angle ε_{xy} which is characteristical for anisotropic material the wing will have an additional twist which can be used to reduce the total elastic angle of attack.

In Fig. 28 the results of parametric studies for different laminates are presented as divergence speed for a fixed geometry.

Case 1 shows that a wing with maximum torsional stiffness (not feasible for strength considerations) has a low divergence speed because the divergence behaviour is mostly influenced by the bending and not the torsional deflection. The laminate of case 2 could fulfill the strength requirements for the aft swept wing of Fig. 26.

WINGBOX SWEEP ANGLE: - 38° LEADING EDGE: - 30°							
CASE		1	2	3	4	5	6
1. LAYER	%	50	50	50	50	70	65
	θ_1	45°	0°	15°	30°	+20°	20°
2. LAYER	%	50	40	40	40	30	25
	θ_2	-45°	±45°	15° ± 45°	30° ± 45°	-70°	70°
3. LAYER	%	-	10	10	10	-	10
	θ_3	-	90°	15° + 90°	30° + 90°	-	65°
DIVERGENCE SPEED	M/SEC	210.	280.	324.	318.	532.	480.
	KTS	408.	544.	630.	618.	1034	933.

FIG. 28 DIVERGENCE SPEED OF A FIXED FSW-GEOMETRY FOR DIFFERENT COMPOSITES

With this laminate a relatively high divergence speed could already be reached. When the main fibre direction is moved forward 15° of the elastic axis (case 3) which gives the anisotropic behaviour of Fig. 27 then the highest divergence speed is reached which reduces when the main fibre direction is forward of the E.A. 30° (case 4). For strength consideration only case 2 and case 3 are feasible. Case 5 and case 6 show that theoretically very high divergence speeds could be achieved but these laminates would give unbearable strength weight penalties. The divergence speed of case 3 is sufficient for a high performance fighter aircraft.

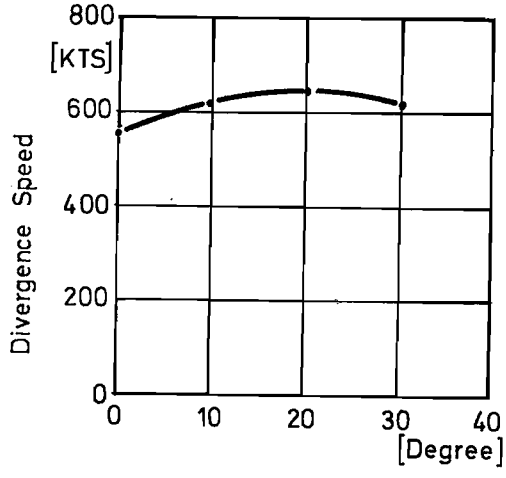

FIG. 29 DIVERGENCE SPEED VERSUS MAIN FIBRE DIRECTION FORWARD OF E.A.

In Fig. 29 the divergence speed is plotted versus the main fibre direction and it shows that the maximum occurs when the direction is about 15° forward of the E.A.

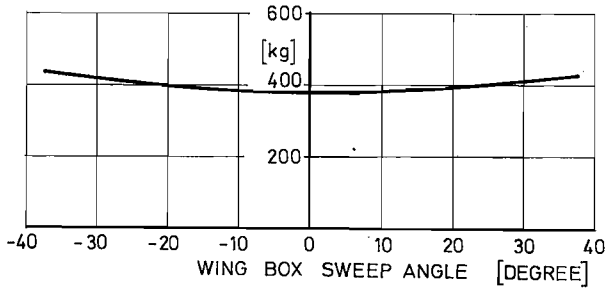

FIG. 30 CFC WING BOX WEIGHT AS A FUNCTION OF SWEEP ANGLE

Fig. 30 shows that there is no weight penalty for a CFC forward swept compared to an aft swept wing.

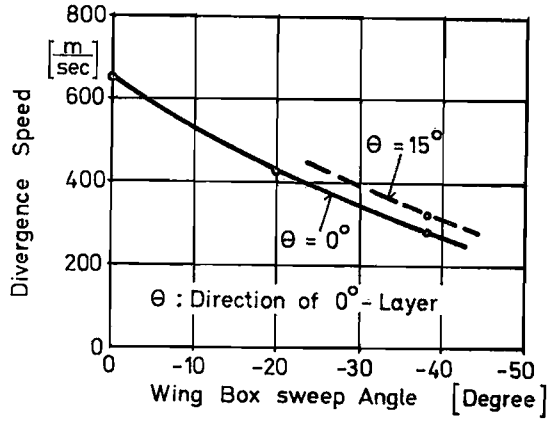

FIG. 31 DIVERGENCE SPEED VERSUS WING BOX SWEEP ANGLE

In Fig. 31 the divergence speed is plotted versus wing box sweep angle for two different main fibre directions. This picture shows how the static divergence speed increases with reducing the wing forward sweep. For a straight wing the divergence speed is above 1300 kts and the flutter speed for this wing would probably be lower.

Conclusions

In this paper it was shown that the very useful structural optimization program ASAT exists at MBB which was used for several practical design studies.

The major advantage of the system is that it merges several airplane designing disciplines such as:

- static loads
- stress calculations
- unsteady aerodynamics
- flutter calculations
- static aeroelastics
- weights

For this reason communication errors are avoided.

Due to the versatility of the computer system separate modules of it can be used solely and it is also possible to make cross checks with results from other structural design groups. CFC structures can be treated efficiently and the design goals postulated from aerodynamic performance could be reached.

The low divergence speed of forward swept wings can be increased sufficiently with no or little weight penalty so that such designs can also be considered for future high performance fighter airplanes.

REFERENCES

1 SENSBURG O., HÖNLINGER H, NOLL T.E.

Active Flutter Suppression on a F-4F Aircraft with External Stores Using Already Existing Control Surfaces

Paper presented at 21st Structures, Structural Dynamics and Materials Conference of the AIAA, 12-14 May 1980, Seattle/Washington, USA

2 WILKINSON K., MARKOWITZ J. et.al.

An Automated Procedure for Flutter and Strength Analysis and Optimization of Aerospace Vehicles

Vol. 1, Theory and Application, AFFDL-TR-75-137

3 GÖDEL H., SCHNEIDER G.

Vergleich des Strukturoptimierungsprogramms FASTOP mit einem Optimierungsprogramm ähnlicher Aufgabenstellung

MBB-internal Report, July 1980

4 SCHNEIDER G.

Aeroelastikuntersuchungen für TKF-SLW

MBB-internal Report, Jan. 1980

5 JOHN H.
Aeroelastik für Delta-Canard
MBB-internal Report

6 GSCHLÖSSL F.
Ergebnisse der statischen Vordimensionierung für den TKF-Delta-Flügel
MBB-internal Report 1980

7 BRÖCKER W.
CFK-Dimensionierungswerte für TKF-Anwendung
MBB-internal Report

8 SCHMIDINGER G.
Lastansätze für Konfiguration 8.18 10 C
MBB-internal Report

9 LÖBERT G.
Aerodynamische Eigenschaften des negativ gepfeilten Flügels
MBB-internal Report 1980

10 WEISSHAAR T.A.
Divergence of Forward Swept Composite Wings
Paper presented at the 20th Structures, Structural Dynamics, and Materials Conference 4-6 April 1979, St. Louis/Mo., USA

11 LANG Beate
Divergenz am Faserverbundflügel
MBB-internal Report 1980

12 LASCHKA B.
Zur Theorie der harmonisch schwingenden tragenden Fläche bei Unterschallströmung
ZfW, Heft 7, 1963

13 FÖRSCHING H.
Grundlagen der Aeroelastik
Springer-Verlag Berlin 1974